© 2016. Published by The Company of Biologists Ltd | Journal of Experimental Biology (2016) 219, 3061-3071 doi:10.1242/jeb.140442

RESEARCH ARTICLE

Do respiratory limitations affect metabolism of insect larvae before moulting? An empirical test at the individual level

Sami M. Kivelä*,‡, Philipp Lehmann and Karl Gotthard

ABSTRACT

Recent data suggest that oxygen limitation may induce moulting in larval insects. This oxygen-dependent induction of moulting (ODIM) hypothesis stems from the fact that the tracheal respiratory system of insects grows primarily at moults, whereas tissue mass increases massively between moults. This may result in a mismatch between oxygen supply and demand at the end of each larval instar because oxygen demand of growing tissues exceeds the relatively fixed supply capacity of the respiratory system. The ODIM hypothesis predicts that, within larval instars, respiration and metabolic rates of an individual larva first increase with increasing body mass but eventually level off once the supply capacity of the tracheal system starts to constrain metabolism. Here, we provide the first individual-level test of this key prediction of the ODIM hypothesis. We use a novel methodology where we repeatedly measure respiration and metabolic rates throughout the penultimate- and final-instar larvae in the butterfly *Pieris napi*. In the penultimate instar, respiration and metabolic rates gradually decelerated along with growth, supporting the ODIM hypothesis. However, respiration and metabolic rates increased linearly during growth in the final instar, contradicting the prediction. Moreover, our data suggest considerable variation among individuals in the association between respiration rate and mass in the final instar. Overall, the results provide partial support for the ODIM hypothesis and suggest that oxygen limitation may emerge gradually within a larval instar. The results also suggest that there may be different moult induction mechanisms in larva-to-larva moults compared with the final metamorphic moult.

KEY WORDS: Critical mass, Growth, Larval instar, Metabolic rate, *Pieris napi*, Respirometry

INTRODUCTION

Insect growth is characterized by moults between larval instars. The developmental physiology of moulting, especially that of the pupal moult, has been elucidated in the model organisms *Drosophila melanogaster* and *Manduca sexta* (Shingleton, 2011; Callier and Nijhout, 2013; Nijhout et al., 2014). Despite differences in the endocrinology of the pupal moult in *D. melanogaster* and *M. sexta* (Shingleton, 2011; Callier and Nijhout, 2013; Nijhout et al., 2014), the key determinants of pupation size and timing are similar in these two species. These are: (1) the critical mass at which pupation (the endocrine cascade preceding moult initiation) is triggered, (2) the duration of growth after the attainment of the critical mass (interval to cessation of growth) and (3) growth rate during the interval to cessation of growth (Nijhout et al., 2006, 2010; Shingleton, 2011). The existence of a critical mass at which pupation is triggered indicates that moult induction is a size-dependent process (Callier and Nijhout, 2011, 2013).

The size-sensing mechanism determining the critical mass is less well understood in the model organisms than the consequent endocrine events, the phenomenon of size-sensing being further obscured by several physiological processes producing some kind of a critical mass. The critical mass (*sensu* Nijhout et al., 2006, 2010; Callier and Nijhout, 2011; Shingleton, 2011) can be seen as a developmental checkpoint where physiological changes are induced (Callier and Nijhout, 2013), potentially associated with constraints for growth. Suggested candidate mechanisms include the limited capacity of the exoskeleton to expand (Bennet-Clark, 1963), potentially hypoallometric growth of the gut, compromising nutrient absorption efficiency (see Esperk and Tammaru, 2004; Grunert et al., 2015), and availability of metabolic intermediates acting as precursors for growth (Callier and Nijhout, 2014). In *D. melanogaster*, the regulation of the critical mass is affected by insulin signalling, the production of prothoracicotrophic hormone and growth of the imaginal discs (Shingleton, 2011, and references therein), so these mechanisms potentially contribute to size-sensing and moult induction. In some insects, abdominal stretch receptors sense body size and induce moulting (Callier and Nijhout, 2013, and references therein). However, in the light of current data, the most plausible mechanism in several species is that limited oxygen supply for growing tissues induces moulting (Greenberg and Ar, 1996; Greenlee and Harrison, 2004, 2005; Callier and Nijhout, 2011). This oxygen-dependent induction of moulting (ODIM) hypothesis stems from the discontinuous growth of the insect tracheal respiratory system. The majority of growth of the tracheal system occurs at moults. Even though some within-instar tracheal growth has been observed in *M. sexta* in the final larval instar (Helm and Davidowitz, 2013), the oxygen supply capacity of the tracheal system apparently cannot follow the continuously increasing oxygen demand of growing tissues for the whole duration of an instar. Accordingly, the minimum oxygen partial pressure required for the maintenance of normal metabolism and feeding increases towards the end of larval instars, which implies that the oxygen safety margin of the respiratory system (i.e. excess oxygen supply capacity) diminishes or even disappears towards the end of larval instars (Greenlee and Harrison, 2004, 2005). In accordance with the ODIM hypothesis, oxygen consumption rate increases with increasing mass before the attainment of the critical mass and becomes mass-independent after the attainment of the critical mass in *M. sexta* (Callier and Nijhout, 2011), which would be expected if the respiratory system is functioning at its maximum capacity after the attainment of the critical mass. Data by Sears et al. (2012; their fig. 3) suggest a qualitatively similar, non-linear pattern in CO_2 emission in *M. sexta*,

Department of Zoology, Stockholm University, Stockholm SE-10691, Sweden.
*Present address: Department of Ecology, University of Oulu, PO Box 3000, Oulu 90014, Finland.

‡Author for correspondence (sami.kivela@oulu.fi)

S.M.K., 0000-0002-6844-9168

Received 14 March 2016; Accepted 19 July 2016

Journal of Experimental Biology (2016) 219, 3061-3071 doi:10.1242/jeb.140442

List of symbols and abbreviations

BIC	Bayesian information criterion
CI	confidence interval
LMM	linear mixed-effects model
MR	metabolic rate
ODIM	oxygen-dependent induction of moulting (hypothesis)
REML	restricted maximum likelihood
RQ	respiratory quotient
SMA	standardized major axis (regression)
SNR	signal to noise ratio
$\dot{V}_{CO_2}$	carbon dioxide production rate
$\dot{V}_{O_2}$	oxygen consumption rate

although data were not analyzed in this respect (but see Greenlee and Harrison, 2005, for a linear pattern in CO_2 emission in *M. sexta*). There may, however, be changes in metabolism affecting oxygen demand and consumption at the critical mass (Callier and Nijhout, 2012, 2014; see also Greenlee and Harrison, 2004). Moreover, Callier and Nijhout (2011) generalized the ODIM hypothesis for all moults between larval instars, as suggested by their data. Finally, a mathematical model derived from the ODIM hypothesis successfully explains moulting sizes in four lepidopteran species (Kivelä et al., 2016), indicating that the ODIM mechanism is a sufficient explanation for moulting sizes in these species.

Not all data are consistent with the ODIM hypothesis. Although low oxygen partial pressure (hypoxia) decreases critical mass both in *D. melanogaster* (Callier et al., 2013) and *M. sexta* (Callier and Nijhout, 2011), as predicted, the expected increase of critical mass under high oxygen partial pressure (hyperoxia) is not seen (Callier et al., 2013). The lack of expected response under hyperoxia does not necessarily refute the ODIM hypothesis because it is possible that other mechanisms start to constrain growth and set the critical mass before the constraint that is due to oxygen supply is met under hyperoxia. It is evident that other mechanisms are involved in moult induction (Callier and Nijhout, 2011; Grunert et al., 2015), but the ODIM mechanism appears to be the dominant one under benign growth conditions.

Empirical tests of the ODIM hypothesis have concentrated on the critical mass. According to the ODIM hypothesis, the critical mass is essentially an individual-level parameter, but because of methodological reasons (Nijhout and Williams, 1974), it has been measured only at the population level so far (Callier and Nijhout, 2011; Callier et al., 2013). Consequently, earlier tests of the ODIM hypothesis must be treated with some caution. Novel individual-level tests are needed for the assessment of the validity of the ODIM hypothesis, and these tests should also have a broader focus and not just concentrate on the critical mass.

Current knowledge allows for an individual-specific approach. The ODIM hypothesis predicts, and the results by Callier and Nijhout (2011) suggest, that the association between oxygen consumption rate and mass should change at the critical mass. As oxygen consumption is closely associated with CO_2 production and metabolic rate in aerobic insects (Wigglesworth, 1972; Downer, 1981), similar changes should be seen in these variables. Respiration rate (with respiration rate we refer to the rate of gas exchange – O_2 consumption or CO_2 production rate – throughout) is expected to first increase with mass but then level off at the critical mass, resulting in a change in the regression slope of respiration rate to mass at the critical mass. Moreover, growth decelerates after attainment of the critical mass because of increasing oxygen limitation to growing tissues, which means that the critical mass is at the inflection point of the instar-specific growth trajectory (Grunert et al., 2015). Limited oxygen supply should also suppress metabolism (Wigglesworth, 1972; Downer, 1981), so that the increase in metabolic rate decelerates towards the end of a larval instar. If there is significant anaerobic metabolism at the end of an instar, the respiratory quotient (RQ; see e.g. Schmidt-Nielsen, 1991) should increase during an instar and eventually overshoot one. Thus, critical mass and oxygen limitation can be inferred from individual trajectories of respiration rate, metabolic rate, growth and RQ. We adopt this novel approach here, but instead of focusing on critical mass, we assess the validity of the ODIM hypothesis at a more general level by analysing whether respiration and metabolic rates increase non-linearly within larval instars, and whether RQ increases towards the end of an instar.

In this study, we repeatedly measure respiration and metabolic rates as well as mass from the same individuals in the non-model green-veined white butterfly *Pieris napi* (Linnaeus 1758). By focusing on within-individual changes in metabolism and growth, we take the necessary methodological step required for a rigorous assessment of the ODIM hypothesis. Specifically, we test the central prediction of the ODIM hypothesis that growth-associated increases in respiration and metabolic rates level off late in larval instars despite continuing growth, because the limited tracheal oxygen supply capacity cannot support increasing whole-organism metabolism until the end of larval instars. This prediction strictly holds only for the growth phase of a larval instar and not for the very end of the instar, when larvae are preparing to moult and are not growing. Therefore, we estimated the potential source of error that may arise because of metabolic changes during the post-growth stage at the very end of an instar. We also estimate changes in RQ as well as body water and lipid content during growth. A changing body composition might influence the relationship between metabolism and body size, and confound the assessment of the ODIM hypothesis.

MATERIALS AND METHODS

Experimental animals

Diapause pupae representing the F_2 laboratory generation of a stock originating from Stockholm (59°22′N, 18°4′E) were exposed to ca. 17°C and 12 h day length to break diapause. Eclosed adults were allowed to mate in flight cages (0.8×0.8×0.5 m) provided with flowers (*Kalanchoe* sp.) and sugar water for feeding in a laboratory with large windows and 400 W metal halide lamps above the cages. Mated females were individually placed into 1 litre containers with *Alliaria petiolata* for oviposition and a piece of cotton wool soaked with sugar water for feeding. A few mated females were kept for 10 days at ca. 5°C before letting them oviposit to produce temporal asynchrony in larval cohorts entering the experiment (these females had *Armoracia rusticana*, *Barbarea vulgaris* and *Brassica napus* as oviposition substrates). Immediately after hatching, F_3 generation larvae were individually transferred to 0.5 litre containers provided with *A. petiolata ad libitum*. Some extra larvae for control measurements (see below) were placed in groups of five individuals into 1 litre containers with *A. petiolata ad libitum*. All larvae were reared under 20°C and 16 h day length (Termaks KBP6395L climate chambers, Termaks, Bergen, Norway) conditions to induce diapause.

Once the singly reared larvae reached the third instar, they were monitored at least twice a day. Larvae were taken to the main experiment immediately when they were observed to have completed the moult to the fourth larval instar. Experimental larvae were divided into two groups: a control group consisting of

Journal of Experimental Biology

Journal of Experimental Biology (2016) 219, 3061-3071 doi:10.1242/jeb.140442

larvae that were weighed twice a day (Precisa XB 120A balance, Precisa, Dietikon, Switzerland) until they became prepupae, and a respirometry group consisting of larvae whose respiration rate and mass were measured twice a day until they became prepupae. All pupae were weighed and sexed ca. 48 h after pupation. Offspring of five females were used in the experiment.

Flow-through respirometry

Carbon dioxide (CO_2) production and oxygen (O_2) consumption of individual larvae were measured to assess metabolic rate using flow-through respirometry. CO_2 production was measured using a Sable Systems (Las Vegas, NV, USA) differential respirometry setup. Two separate lines of outdoor air scrubbed of H_2O and CO_2, using Drierite (W. A. Hammond Drierite, Xenia, OH, USA) and ascarite (Acros Organics, USA) scrubbers, respectively, were pushed at a steady rate of 150 ml min^{-1} using two separate mass flow controllers (840 Series; Sierra Instruments, Monterey, CA, USA). Flow was generated using a SS-4 pump (Sable Systems) set to 500 ml min^{-1}. The first line then went into a MUX multiplexer (Sable Systems) and through the measurement chamber (volume 10 ml), which was placed in a climate cabinet (Panasonic MIR-154-PE, Panasonic, Osaka, Japan) set to 20°C, after which it again was scrubbed of H_2O with Drierite and then entered the sample line of an Li-7000 CO_2 analyser (LiCor, Lincoln, NE, USA). The second line proceeded the same way, mimicking the exact length of the sample line (including an empty measurement chamber), entering the reference line of the Li-7000 CO_2 analyser. The lines then proceeded through a second set of ascarite CO_2 scrubbers and entered an Oxzilla FC-2 O_2 analyser (Sable Systems), after which air was ejected to the room. Preliminary measurements were performed to ensure stability of flow rate through either channel by measuring the flow rate of air ejected from the O_2 analyser. Differential CO_2 and O_2 were calculated by subtracting the output of the reference line from the output of the sample line. For all measurements, sampling rate was 1 Hz. The measurement protocol entailed a 3 min baseline measurement of an empty chamber, then a 10 min measurement of the chamber containing the animal, and finally a repeat 3 min measurement of the empty chamber. The raw output was baseline corrected against the empty chamber value, fractioned and multiplied with flow rate to yield ml CO_2 or O_2 h^{-1} (Lighton, 2008).

Larvae were without food during the measurement that lasted 16 min in total, but were not starved before the measurements to avoid negative effects on growth (see Results). During the measurement, movement as well as the number of frass produced was recorded through visual inspection through the glass wall of the measurement chamber. The chamber was divided into three equally sized compartments and number of movements between compartments was recorded. Larvae were weighed after the measurements.

Syringe-flow respirometry

Syringe-flow respirometry was used to estimate RQ for fourth-instar larvae, because preliminary tests indicated that flow-through estimates of O_2 consumption are not reliable for this instar. In total, 28 singly and group-reared fourth-instar larvae were taken at different stages of the instar and individually enclosed in 20 ml syringes filled with humid air within a volume of 4 ml at 20°C. After approximately 2 h, 3 ml air from the syringe was blown to the Li-7000 CO_2 analyser followed by the Oxzilla FC-2 O_2 analyser with the same setup as used in flow-through respirometry. Each larva was measured only once.

Calculating metabolic rates

We used respirometry data to calculate metabolic rate (MR; W). MR was calculated as $MR=(X\times\dot{V}_{O_2})/3600$, where $X=15.97+(5.164\times RQ)$ is the oxyjoule equivalent (J ml^{-1} O_2) and RQ is the respiratory quotient [$\dot{V}_{CO_2}/\dot{V}_{O_2}$, where $\dot{V}_{CO_2}$ is the CO_2 production rate (ml CO_2 h^{-1}) and $\dot{V}_{O_2}$ is the O_2 consumption rate (ml O_2 h^{-1})] (see Lighton et al., 1987). The denominator, 3600 s (1 h=3600 s), converts MR into W (i.e. J s^{-1}).

In the fourth larval instar, $\dot{V}_{O_2}$ was calculated as $\dot{V}_{fCO_2}/0.78$, where $\dot{V}_{fCO_2}$ is the individual-specific flow-through estimate for CO_2 production rate, and the denominator is the syringe-flow estimate for RQ in this instar. In the fifth larval instar, we used the individual-specific flow-through estimates for both RQ and $\dot{V}_{O_2}$ when calculating MR. We assessed how sensitive the instar-specific mean MRs were for the used RQ value by repeating the calculations with a sequence of RQ values varying from 0.9 times the estimate to 1.1 times the estimate, the estimate being 0.78 for instar IV and 0.89 for instar V. Note that the same RQ value was used for all fifth-instar larvae in the sensitivity analysis instead of the individual-specific ones used in the analysis of MR.

Starvation control

To estimate the effects of starvation on metabolic rate, we repeatedly measured metabolic rate during starvation from four fourth-instar and four fifth-instar group-reared larvae that represented different stages of the two instars. The MR of each individual was measured with the flow-through method (see above) after feeding, and thereafter at 1 h intervals under starvation until 4 h of starvation.

Water and total lipid extraction

Water and total lipid content of larvae were measured after chloroform:methanol (Chl:Meth) extraction (Folch et al., 1957) according to the following protocol. Group-reared larvae were frozen at −20°C individually during the penultimate and ultimate instars. After freezing, they were weighed (fresh mass; Precisa XB 120A balance), five holes were punctured with a sterile needle along the lateral sides of the larvae when still frozen, and then they were dried for 72 h at 55°C. Larvae were then reweighed (dry mass) and placed in small glass vials (20 ml) containing 5 ml Chl:Meth (2:1 v:v) for 72 h in a fume hood at 20°C. Chl:Meth effectively dissolves lipids in the sample into the liquid phase. This includes neutral lipids and phospholipids, but also glycerol, carbohydrates and amino acids (Newman et al., 1972), so this method overestimates total lipids (Williams et al., 2011). In our case, unpublished data suggest no significant glycerol content in the larvae (P.L., personal observations). After the Chl:Meth submersion, larvae were dried for another 24 h at 55°C and weighed (lean mass). Total water content (percentage) was calculated by dividing the difference between fresh and dry mass by fresh mass and multiplying by 100%. Total lipid content (percentage) was calculated by subtracting lean mass from dry mass, dividing by fresh mass and multiplying by 100%.

Statistical analyses

All statistical analyses were conducted with R version 3.2.2 (https://www.R-project.org/). Scaling of CO_2 production rate, O_2 consumption rate and MR to body mass was analyzed with standardized major axis (SMA) regression (function 'sma'; Warton et al., 2012) of ln-transformed trait values on ln-transformed mass. Because our data consisted of repeated measurements on the same individuals, we avoided the problem of non-independence of observations by conducting a resampling analysis. Ten thousand resamples were generated so that a single observation was randomly

Journal of Experimental Biology (2016) 219, 3061-3071 doi:10.1242/jeb.140442

derived from each individual in each round of resampling. An SMA regression model was fitted to each of the 10,000 subsets of data consisting only of independent observations (i.e. each individual represented only once in the data sets). Confidence intervals of the SMA slopes were approximated with the percentile method (i.e. 95% CI limits are 0.025 and 0.975 percentiles; Davison and Hinkley, 1997).

Control larvae were weighed at similar intervals as the experimental larvae whose MRs and masses were repeatedly measured. There were 20 control larvae, 19 of which survived until pupation. In the respirometry group, CO_2 production rate, O_2 consumption rate (instar V only; see below) and MR were analyzed in fourth and fifth larval instars both by (1) including all observations of the focal instar, and (2) including only the periods when somatic growth takes place, meaning that moulting (and preparation for moulting) and wandering (after the attainment of peak mass in the fifth instar) stages were excluded from the latter analyses. We obtained complete data (including information on sex, i.e. survival until pupation) on 19 (out of 22) individuals, resulting in 137 and 227 measurements (96 and 191 for growth only data) on fourth- and fifth-instar larvae, respectively. On average, there were 7.02 and 11.9 measurements (5.05 and 10.1 for growth only data) per individual in the two respective instars.

All measurements of CO_2 production rate had very high signal to noise ratios (SNR), indicating a strong biological signal in this variable. For the analysis of O_2 consumption rate (and MR in the fifth instar), we included only measurements where SNR was ≥5, because a low SNR indicates a weak biological signal. SNR was calculated for individual O_2 measurements by dividing the difference between mean $\dot{V}_{O_2}$ of the animal and empty chamber with the standard deviation of the mean $\dot{V}_{O_2}$ of the empty chamber. Our SNR threshold precluded analysis of O_2 consumption rate in the fourth instar (three out of 137 measurements exceeded the threshold). In the final instar, the majority of measurements (188 out of 227) exceeded the SNR threshold. Owing to this, we analyzed variation in RQ only in the final instar. Note, however, that we could calculate MR accurately in both investigated instars (see Calculating metabolic rates, above, and Results sections).

Respirometry data were analyzed with linear mixed-effects models (LMMs) fitted with the restricted maximum likelihood (REML) method (function 'lme'; R package 'nlme' by J. Pinheiro, D. Bates, S. DebRoy, D. Sarkar and R Core Team, version 3.1-121, http://CRAN.R-project.org/package=nlme). The response variables (CO_2 production rate in instars IV and V, O_2 consumption rate in instar V, and MR in instars IV and V) were standardized by subtracting the mean and by dividing with the standard deviation to aid model convergence, and to reduce random effect correlations. Fixed effects initially included standardized mass, the square of standardized mass, sex, movement within the measurement chamber (number of crossing borders between three equal-sized parts of the measurement chamber), number of frass produced during the measurement and timing of the measurement in the diel cycle. The interactions between sex and each of standardized mass and square of standardized mass were also initially included in fixed effects. First, the best random effect structure was found by keeping the fixed effects constant in the form described above, and comparing alternative models with different random effects on the grounds of likelihood ratio tests and the Bayesian information criterion (BIC). The alternative random effect formulations included (1) random individual-specific intercepts and coefficients for standardized mass and squared standardized mass, (2) random individual-specific intercepts and coefficients for standardized mass, and (3) random individual-specific intercepts only. The initial models were heteroschedastic, which was taken into account by adding an exponential variance function 'varExp' (R package 'nlme') with the fitted value as the variance covariate to the models. The random effect structure (2) was best for all analyzed variables in the fourth larval instar (ΔBIC>2.8 in all comparisons including the best random effect structure), whereas random individual-specific intercepts (3) sufficed for all variables in the fifth larval instar (ΔBIC>2.3). Second, fixed effects were reduced by hierarchically removing insignificant terms (removals were supported by BIC). Model goodness-of-fit was visually evaluated from residual plots.

Variation in RQ in the fifth larval instar was analyzed similarly as in other respirometry variables, except that the fixed effects initially included standardized mass, the square of standardized mass, sex, timing of the measurement and an indicator variable 'stage' (growth stage/wandering stage). The interactions between sex and each of standardized mass and square of standardized mass were initially included in fixed effects. The response variable was not standardized to aid interpretation of the results as the RQ value as such is of interest. The random effect structure (3) was best (ΔBIC>8.3), and no variance function was needed.

The ODIM hypothesis predicts that the relationship between MR and mass changes at an instar-specific critical mass where O_2 supply begins to constrain growth. The results of Callier and Nijhout (2011) imply a linear increase in MR with increasing mass before the attainment of the critical mass, and a mass-independence of MR after the attainment of the critical mass. Thus, the slope of the regression of respiration rate on mass is expected to change from positive to zero at the critical mass. Therefore, we investigated the relationship between CO_2 production rate and mass during growth in the fifth larval instar separately for each individual with a segmented regression analysis (function 'segmented'; Muggeo, 2008). We set starting value for the breakpoint to be 100 mg and the parameter h to equal 0.14 (the analysis did not succeed for each individual with higher values).

Data from the starvation control were analyzed with LMMs fitted with the REML method (function 'lme'; R package 'nlme'). The response variable was mass-specific rate of CO_2 production and individual identity was set as a random effect (i.e. random individual-specific intercepts). Fixed effects initially included time since the beginning of starvation, its square, larval instar, and interactions between larval instar and each of linear and squared time since the beginning of starvation. An exponential variance function 'varExp' (R package 'nlme') with the fitted value as the variance covariate was added to the model to take heteroschedasticity into account. Fixed effects were reduced by hierarchically removing insignificant terms (removals were supported by BIC).

Body composition data were analyzed with linear models (function 'lm'). Variation in relative water and lipid content (percentage) was explained with fresh mass and instar (IV/V). Interaction between fresh

Table 1. Allometric scaling exponents (standardized major axis regression slopes, 95% confidence intervals in parentheses; derived from a resampling analysis; see 'Statistical analyses' section of Materials and methods for details) of the measured traits in relation to body mass in fourth and fifth larval instars in *Pieris napi*

Variable	Instar	Whole-instar data	Growth-only data
CO_2 production	IV	0.814 (0.605, 1.04)	0.990 (0.776, 1.21)
Metabolic rate	IV	0.814 (0.605, 1.04)	0.990 (0.776, 1.21)
CO_2 production	V	1.00 (0.842, 1.19)	1.05 (0.920, 1.19)
O_2 consumption	V	0.928 (0.704, 1.26)	0.925 (0.738, 1.17)
Metabolic rate	V	0.936 (0.729, 1.24)	0.934 (0.771, 1.15)

Journal of Experimental Biology (2016) 219, 3061-3071 doi:10.1242/jeb.140442

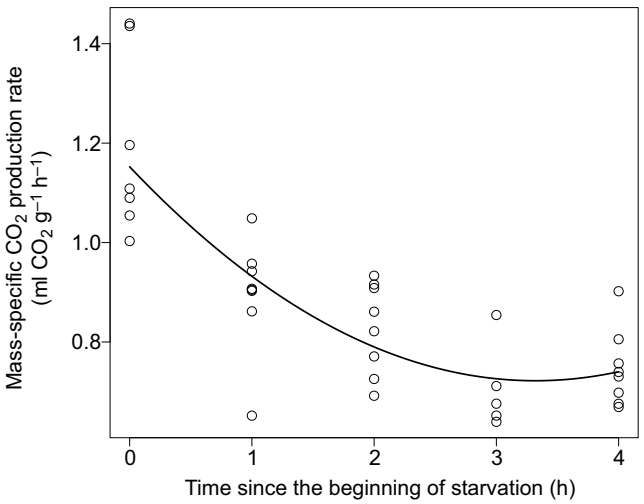

Fig. 1. Mass-specific CO_2 production rate in relation to starvation time in *Pieris napi*. The curve is a fitted quadratic regression derived from the linear mixed-effects model analysis (see 'Statistical analyses' section of Materials and methods for details). The regression equation is $y=1.15-0.259x+0.0391x^2$, where y refers to mass-specific CO_2 production rate and x to starvation time. Both the linear and quadratic terms of time were statistically significant (linear term: $t_{26}=-5.67$, $P<0.0001$; quadratic term: $t_{26}=4.42$, $P=0.0002$).

mass and instar was initially included in the models, and insignificant (risk level 0.05) terms were hierarchically removed.

RESULTS

Scaling of the measured variables to body size

Isometric scaling between the measured traits (CO_2 production, O_2 consumption and MR) and body mass could not be excluded in any cases as all 95% confidence intervals of the scaling exponents encompassed 1 (Table 1). In the fourth instar, the estimated scaling exponents were higher – and very close to 1 – when growth-only data were used compared with the case where all data from this instar were used in the analysis (Table 1).

Comparison between experimental and control groups

There was no difference in development times (time until peak mass: $t_{35.39}=-1.32$, $P=0.20$; time until pupation: $t_{33.89}=-1.46$, $P=0.15$) or final masses (peak mass: $t_{36.99}=0.574$, $P=0.57$; pupal mass: $t_{34.94}=0.462$, $P=0.65$) between the experimental and control groups, indicating that there was no added stress of respirometric measurements compared with mere weighing.

Effect of starvation on metabolism

We investigated the metabolic consequences of our respirometry protocol in the starvation experiment. There was a non-linear decline in the mass-specific CO_2 production rate in relation to starvation time (linear term: $F_{1,26}=39.9$, $P<0.0001$; quadratic term: $F_{1,26}=19.5$, $P=0.0002$); mass-specific CO_2 production rate declined steeply in the beginning of starvation and stabilised after ca. 3 h of starvation (Fig. 1). Hence, standardization of the pre-respirometry handling of the larvae is necessary. Our choice of no starvation before respirometric measurements was, thus, justified, particularly as we avoided adverse effects on growth that way (see Comparison between experimental and control groups, above).

Association between metabolism and growth

In the fourth larval instar, there was a non-linear relationship between CO_2 production rate and mass (Table 2, Fig. 2), the increase in CO_2 production rate gradually weakening and eventually levelling off with increasing mass, as predicted by the ODIM hypothesis. The levelling off was stronger when preparation for moulting was included in the analysis (Tables 2, 3), predicted CO_2 production rate even decreasing with increasing mass at the end of the instar (Fig. 2). Females had a slightly higher CO_2 production rate than males (Tables 2, 3, Fig. 2). The results concerning MR parallel those of CO_2 production rate in the fourth larval instar (Table 4, Fig. 3).

In the fifth larval instar, the relationship between CO_2 production rate and mass was non-linear with some levelling off at the end of the instar when the wandering stage was included in the analysis (Table 2, Fig. 2). However, the non-linearity disappeared when the wandering stage was excluded from the analysis, and a line with a

Table 2. Fixed effects of linear mixed-effects models explaining variation in the (standardized) rates of CO_2 production in the fourth (IV) and fifth (V) larval instars as well as the (standardized) rate of O_2 consumption and (unstandardized) respiratory quotient (RQ) in the fifth larval instar in *Pieris napi*

Variable	Parameter	Estimate	s.e.	d.f.	t	P
CO_2 production IV[a]	Intercept	0.641	0.139	115	4.62	<0.0001
	Std. mass	0.532	0.100	115	5.32	<0.0001
	Std. mass^2	−0.545	0.0579	115	−9.42	<0.0001
	Sex (male)	−0.266	0.0907	17	−2.93	0.0093
	Movement	−0.101	0.0420	115	−2.41	0.017
CO_2 production V[b]	Intercept	0.0416	0.0445	205	0.936	0.35
	Std. mass	0.735	0.0433	205	17.0	<0.0001
	Std. mass^2	−0.0797	0.0297	205	−2.68	0.0080
	Sex (male)	−0.0909	0.0395	17	−2.30	0.034
	Frass	0.210	0.0641	205	3.28	0.0012
O_2 consumption V[b]	Intercept	−0.154	0.0554	167	−2.77	0.0062
	Std. mass	0.678	0.0403	167	16.8	<0.0001
	Frass	0.437	0.0980	167	4.46	<0.0001
RQ V[b]	Intercept	0.902	0.0169	166	53.3	<0.0001
	Std. mass	0.0203	0.0104	166	1.82	0.071
	Std. mass^2	−0.0313	0.0104	166	−3.01	0.003
	Stage (wandering)	−0.0668	0.0272	166	−2.46	0.015

Post-growth stages are included.
[a]Random effects include random individual-specific intercepts and coefficients for standardized mass.
[b]Random effects include random individual-specific intercepts.

Journal of Experimental Biology (2016) 219, 3061-3071 doi:10.1242/jeb.140442

Table 3. Fixed effects of linear mixed-effects models explaining variation in the (standardized) rates of CO_2 production in the fourth (IV) and fifth (V) larval instars as well as the (standardized) rate of O_2 consumption in the fifth larval instar during growth in *Pieris napi*

Variable	Parameter	Estimate	s.e.	d.f.	*t*	*P*
CO_2 production IV[a]	Intercept	0.311	0.0895	75	3.48	0.0008
	Std. mass	0.917	0.0742	75	12.4	<0.0001
	Std. mass^2	−0.248	0.0398	75	−6.24	<0.0001
	Sex (male)	−0.210	0.0870	17	−2.42	0.027
CO_2 production V[b]	Intercept	0.00417	0.0379	170	0.110	0.91
	Std. mass	0.893	0.0255	170	35.1	<0.0001
	Sex (male)	−0.0947	0.0426	17	−2.22	0.040
	Frass	0.126	0.0531	170	2.37	0.019
O_2 consumption V[b]	Intercept	−0.356	0.116	133	−3.06	0.0027
	Std. mass	0.849	0.0360	133	23.6	<0.0001
	Frass	0.222	0.0778	133	2.85	0.0050
	Time	0.458	0.173	133	2.65	0.0091

Post-growth stages are excluded.
[a]Random effects include random individual-specific intercepts and coefficients for standardized mass.
[b]Random effects include random individual-specific intercepts.

positive slope best described the relationship between CO_2 production rate and mass (Table 3, Fig. 2), contradicting the prediction of the ODIM hypothesis. Females had a slightly higher CO_2 production rate than males (Tables 2, 3, Fig. 2). The number of frass produced during the measurement entered the final model, indicating increasing CO_2 production with increasing number of frass produced (Tables 2, 3).

The overall results concerning O_2 consumption rate in the fifth larval instar were quite similar to those for CO_2 production rate, except that the relationship between O_2 consumption rate and mass was linear even when wandering stage was included in the analysis, but the slope become steeper with the exclusion of the wandering stage (Tables 2, 3, Fig. 2). The time of the measurement in relation to the diel cycle entered the final model when wandering stage was excluded. O_2 consumption rate increased slightly with increasing movement and towards the evening (Table 3), and it was positively correlated with the number of frass produced during the measurement independently of the inclusion/exclusion of the wandering stage (Tables 2, 3).

Results concerning variation in metabolic rate in the fifth larval instar are very similar to those of O_2 consumption rate in the same instar (compare Table 4 with Tables 2 and 3, and Fig. 3 with Fig. 2). The parameters of statistical models explaining variation in MR in fourth and fifth larval instars are insensitive to the RQ value used in calculating MRs, because standardized values were used in statistical analyses. Even (unstandardized) mean metabolic rates in the two instars are relatively insensitive to up to 10% changes in the reference RQ value (Fig. S1).

In the fifth larval instar, RQ first increased during growth but slightly declined at the end of the growth stage (Table 3, Fig. 4). RQ was lower during the wandering stage than during growth (Table 3, Fig. 4). The highest RQ values exceeded 1, as expected, but were not associated with large body size (Fig. 4), which contradicts the prediction. The RQ values suggest that larvae mainly burn lipids in the beginning of the instar, rely more on carbohydrates during the rest of the growth stage, and slightly increase the use of lipids as a fuel in the wandering stage.

Individual-specific analysis

Segmented regression analysis revealed individual-level variation in the relationship between CO_2 production rate and mass in the fifth instar (Fig. 5). Some individuals showed the predicted pattern where

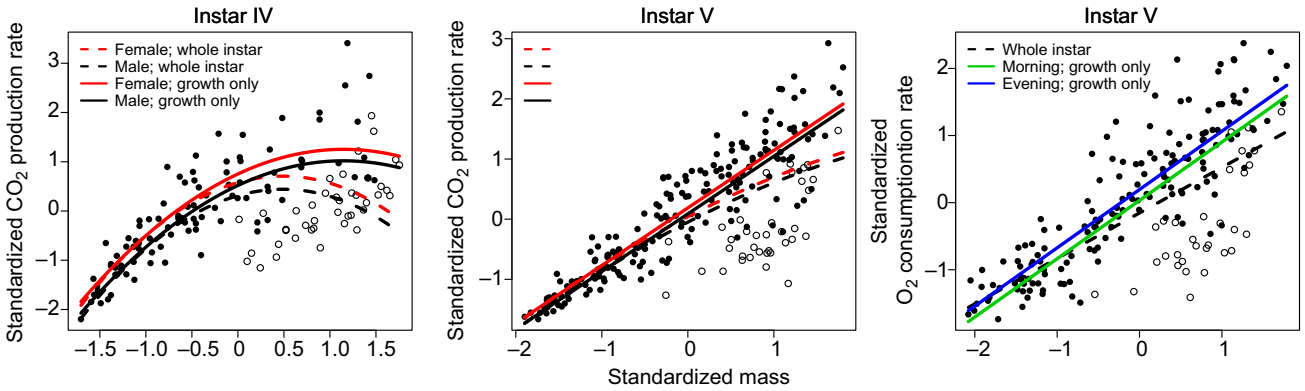

Fig. 2. Standardized CO_2 production rate in fourth and fifth larval instars and standardized O_2 consumption rate in the fifth larval instar in relation to standardized larval mass in *Pieris napi*. Closed and open circles indicate observations during the growth and post-growth (instar IV: non-feeding stage preparing for moulting; instar V: wandering stage) stages, respectively. Curves/lines depict fitted regressions from the mixed-effects model analyses (dashed lines for analyses including all observations; continuous lines for analyses including only growth period). Movement during the measurement entered the final model for all fourth instar data, and mean movement was used in drawing the regression curves. Number of frass entered all the final models for fifth instar data, and the presented regression curves/lines were drawn for the most common case of no frass produced during the measurement. The regression lines for standardized O_2 consumption rate in the growth period during the fifth larval instar are presented for the mean morning and evening measurement times and for the mean movement activity during the measurement. For the purpose of illustration and comparison, the regression curves/lines for growth stages (continuous lines) presented here were derived using the growth stage subset of the values of standardized variables in the data including also the post-growth observations.

Journal of Experimental Biology

Journal of Experimental Biology (2016) 219, 3061-3071 doi:10.1242/jeb.140442

Table 4. Fixed effects of linear mixed-effects models explaining variation in (standardized) metabolic rates in the fourth (IV) and fifth (V) larval instars in *Pieris napi*

Data set	Parameter	Estimate	s.e.	d.f.	*t*	*P*
Instar IV; all data[a]	Intercept	0.641	0.139	115	4.62	<0.0001
	Std. mass	0.532	0.100	115	5.32	<0.0001
	Std. mass^2	−0.545	0.0579	115	−9.42	<0.0001
	Sex (male)	−0.266	0.0908	17	−2.93	0.0094
	Movement	−0.101	0.0420	115	−2.41	0.017
Instar IV; growth only[a]	Intercept	0.311	0.0895	75	3.48	0.0008
	Std. mass	0.917	0.0742	75	12.4	<0.0001
	Std. mass^2	−0.248	0.0398	75	−6.24	<0.0001
	Sex (male)	−0.210	0.0870	17	−2.42	0.027
Instar V; all data[b]	Intercept	−0.145	0.0533	167	−2.71	0.0074
	Std. mass	0.694	0.0372	167	18.7	<0.0001
	Frass	0.394	0.0923	167	4.27	<0.0001
Instar V; growth only[b]	Intercept	−0.318	0.102	133	−3.13	0.0022
	Std. mass	0.859	0.0324	133	26.6	<0.0001
	Frass	0.205	0.0698	133	2.93	0.0039
	Time	0.396	0.150	133	2.65	0.0091

[a]Random effects include random individual-specific intercepts and coefficients for standardized mass.
[b]Random effects include random individual-specific intercepts.

CO_2 production rate first increases with increasing mass, but levels off in the latter part of the instar (Fig. 5). Some other individuals showed the opposite pattern, MR increasing more steeply in relation to mass in the end than in the beginning of the instar (Fig. 5). The confidence intervals for the estimated regression slopes and slope breakpoints were too wide for inferences, apparently because the number of individual-specific data points was relatively low. The main message is, however, that there may be considerable individual-level variation (including non-linear responses) even though population-level data show a consistent (linear) pattern.

Changes in body composition during growth

Relative water content of the larvae decreased with increasing body size (univariate regression: R^2=0.747, $F_{1,\ 31}$=91.3, P<0.0001; Fig. 6A), but instar or the interaction between instar and fresh mass did not enter the final model. On average, relative water content was lower in the fifth than in the fourth instar (mean IV=86.8%, 95% CI=85.9–87.6%; mean V=83.6%, 95%CI=82.4–84.8%). Relative lipid content showed the opposite pattern. It increased with increasing body size (univariate regression: R^2=0.720, $F_{1,25}$=64.4, P<0.0001; Fig. 6B), neither instar nor the interaction between instar and fresh mass entering the final model in this case either. Lipid content was higher in the fifth than in the fourth instar (mean IV=1.26%, 95%CI=0.0980–2.43%; mean V=2.84%, 95% CI=2.36–3.33%).

DISCUSSION

The individual-specific approach used in the present study revealed that respiration rate and MR gradually decelerate towards the end of the growth stage in the penultimate (IV) larval instar in *P. napi*, as predicted by the ODIM hypothesis. This deceleration does not appear to be a consequence of hypoallometric scaling of respiration and metabolism to body mass because these traits scaled isometrically to body size over the growth period (i.e. excluding

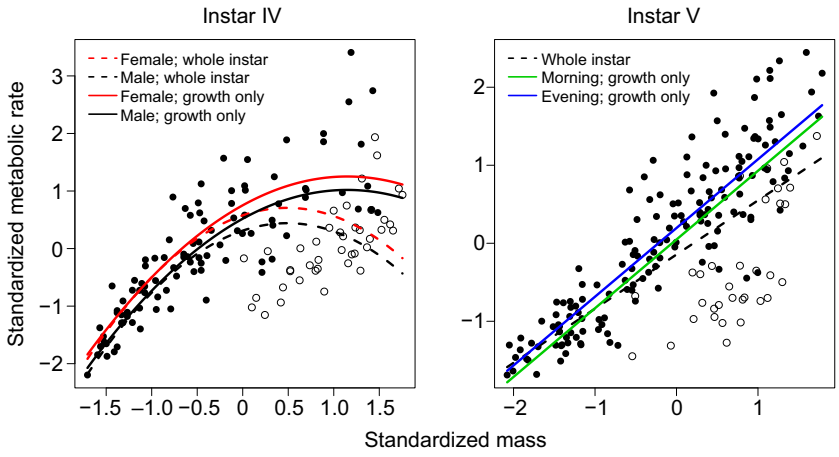

Fig. 3. Standardized metabolic rate in fourth and fifth larval instar in relation to standardized larval mass in *Pieris napi*. Closed and open circles indicate observations during the growth and post-growth (instar IV: non-feeding stage preparing for moulting; instar V: wandering stage) stages, respectively. Curves/lines depict fitted regressions from the mixed-effects model analyses (dashed lines for analyses including all observations; continuous lines for analyses including only growth period). Movement during the measurement entered the final model for all fourth instar data, and mean movement was used in drawing the regression curves. Number of frass entered all the final models for fifth instar data, and the presented regression curves/lines were drawn for the most common case of no frass produced during the measurement. The regression lines for standardized metabolic rate in the growth period during the fifth larval instar are presented for the mean morning and evening measurement times. For the purpose of illustration and comparison, the regression curves/lines for growth stages (continuous lines) presented here were derived using the growth-stage subset of the values of standardized variables in the data including also the post-growth observations.

Journal of Experimental Biology (2016) 219, 3061-3071 doi:10.1242/jeb.140442

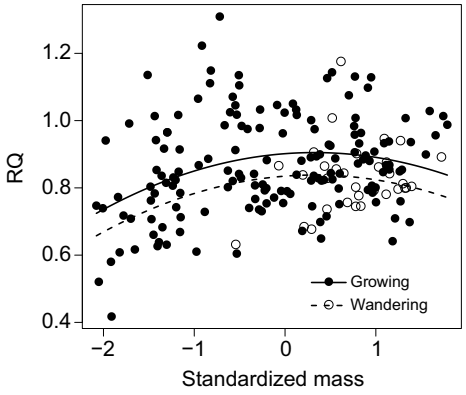

Fig. 4. Respiratory quotient (RQ) in growing (closed circles, continuous line) and wandering (open circles, dashed line) fifth-instar *Pieris napi* larvae in relation to standardized mass. Curves depict fitted regressions from the mixed-effects model analysis.

moulting) of the focal instar. Still, it remains possible that the scaling varies within the growth period. A rigorous test of the ODIM hypothesis requires that only growth-stage observations are included in the analysis because oxygen limitation should become apparent during growth, whereas respiration and metabolism may be reduced by other reasons during moulting (cf. Camp et al., 2014) (Figs 2 and 3). The importance of including only growth-stage data in tests of the ODIM hypothesis is highlighted by the sensitivity of conclusions to the inclusion of post-growth data in the final (V) larval instar. Growth-stage data from the final instar were not consistent with the ODIM hypothesis as respiration rate and MR increased linearly with increasing mass throughout the growth stage and the scaling of these traits to body size were isometric. However, inclusion of all observations (including the wandering stage) produced results consistent with the ODIM hypothesis in CO_2 production rate in the final instar, but this consistency with predictions is likely to be an artefact of the relatively low respiration rate and MR during the wandering stage. Hence, respiration data do not support the ODIM hypothesis in the final larval instar in *P. napi*. The difference between larval instars found here is not consistent with population-level data on *M. sexta*, where all three studied larval instars show a pattern consistent with the ODIM hypothesis (Callier and Nijhout, 2011). Our results concerning MR also seem reliable as results remain unchanged regardless of whether individual or group RQ values are used in the

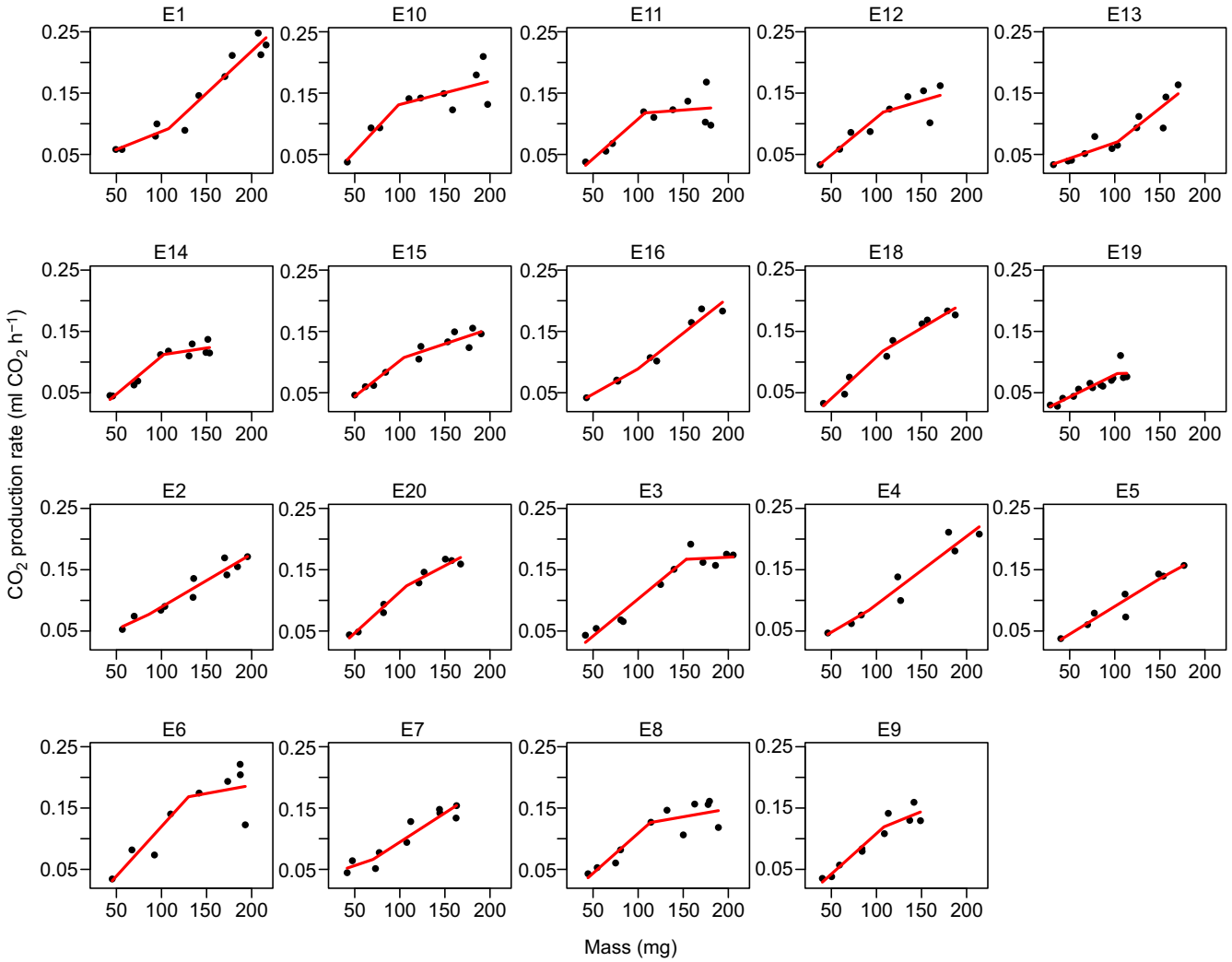

Fig. 5. Fitted individual-specific segmented regression lines (red lines) for the rate of CO_2 production versus mass and the observations (points) in the fifth larval instar in *Pieris napi*. Each panel is for a single individual.

Journal of Experimental Biology

Journal of Experimental Biology (2016) 219, 3061-3071 doi:10.1242/jeb.140442

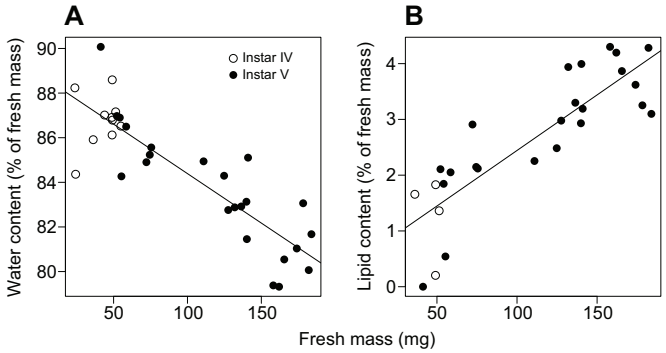

Fig. 6. Relative water and lipid content (percentage of fresh mass) in relation to fresh mass in fourth- (open circles) and fifth-instar (closed circles) *Pieris napi* larvae. Regression lines fitted to the combined data of both instars are shown. The regression equations are: (A) $y_{\text{water content}}=88.8-0.0443x$ and (B) $y_{\text{lipid content}}=0.451+0.0199x$, where x refers to fresh mass.

MR calculation (Fig. S1). These data thus support the use of general reference RQ values when individual-specific values are not available (Lighton, 2008).

The ODIM hypothesis states that the tracheal system oxygen supply capacity sets an upper limit for respiration rate and MR within an instar, because the tracheal system is relatively fixed for the whole duration of an instar. Even if there is some within-instar tracheal growth in final-instar *M. sexta* (Helm and Davidowitz, 2013), it is unlikely to compensate for the rapid increase in oxygen demand during exponential tissue growth before the instar-specific critical mass (cf. Nijhout et al., 2006; Grunert et al., 2015). In fact, tracheal volume, which is typically assumed to correlate positively with oxygen supply capacity, decreases within earlier instars in *M. sexta* (Callier and Nijhout, 2011) and in fifth-instar *Schistocerca americana* apparently because growing tissues compress tracheae (Lease et al., 2006). According to the ODIM hypothesis, moulting is triggered at the critical mass at which oxygen demand meets the supply capacity, but growth still continues after it, although with a decelerating rate until the cessation of growth for moulting (or entering the wandering stage in the final instar) (Nijhout et al., 2006; Grunert et al., 2015). At the cessation of growth, the gut is purged and moulting begins (except in the final instar where the wandering stage begins after gut purging), which results in changes in MR independently of the ODIM mechanism (cf. Camp et al., 2014) (Figs 2 and 3). Therefore, it is necessary to exclude post-growth observations when testing the ODIM hypothesis, as we did here. As we demonstrated, the inclusion of post-growth observations may result in erroneous conclusions, but this potential source of error has not been considered earlier (see Callier and Nijhout, 2011).

When considering growth-only data, the penultimate larval instar results were consistent with the ODIM hypothesis but the final instar results were not. This difference between larval instars is surprising, and our data do not suggest any explanations for it. The two larval instars, however, differ in an important aspect. The penultimate instar is primarily used for growth, whereas the final instar encompasses both growth and preparation for metamorphosis. The endocrinology underlying moulting also differs between the two instars in *M. sexta* (Callier and Nijhout, 2013; Nijhout et al., 2014). Moreover, there are differences in body composition between the penultimate and final larval instars as water content is lower and lipid content higher in the final than in the penultimate instar, suggesting that the majority of lipid reserves accumulate during the final instar (see also Ojeda-Avila et al., 2003). The RQ values in our final-instar data (Fig. 4) further suggest that body lipid is the main fuel for metabolism only in the very beginning of the instar, when the larvae are probably in a state corresponding to starvation after the previous moult. Later in the instar, carbohydrates appear as the main fuel for metabolism and body lipid rather functions as energy reserve for later development, or diapause, as in the current case (Hahn and Denlinger, 2007). The highest RQ values were $1<RQ<1.3$, which may indicate either partially anaerobic metabolism (e.g. Nielsen and Christian, 2007) or conversion of dietary carbohydrates to lipids (Zebe, 1953; Wigglesworth, 1972). The increasing body lipid content during the final instar (Fig. 6B) suggests that lipid synthesis is the most likely explanation for the RQ values exceeding 1 in our data. An increasing mass of metabolically inactive lipid may postpone the point at which tracheal oxygen supply starts limiting metabolism. Even if this is the case, oxygen limitation should still become realised at some point in final-instar larvae if the ODIM hypothesis holds true, and this seems to be the case in *M. sexta*, where the indication for oxygen limitation is strongest late in the final larval instar (Callier and Nijhout, 2012). It would actually pay to start building lipid reserves after the attainment of the critical mass in each instar because of the low metabolic needs for the maintenance of lipid tissue. Data on final-instar *M. sexta* lipid content imply that this may indeed be the case (Ojeda-Avila et al., 2003).

Even though our data on the final larval instar are not consistent with the ODIM hypothesis, we cannot completely refute the hypothesis for final-instar *P. napi*. Our approach reveals individual-level variation in the association between respiration rate and mass as some final-instar larvae show the expected pattern of respiration rate levelling off late in the growth period, while other individuals show an almost linear increase in respiration rate through the instar, and some individuals even show an accelerating increase in respiration rate with increasing mass (Fig. 4). Yet, it is currently not completely clear whether a levelling off in respiration rate late in an instar would represent oxygen limitation, as mass-specific oxygen demand decreases within instars (Callier and Nijhout, 2012), and mass-independency of respiration rate in growing larvae may not necessarily be caused by oxygen limitation (Callier and Nijhout, 2014). However, the low numbers of individual-specific data points preclude rigorous inferences concerning our individual-level analysis, but the results suggest that some individuals reach a critical mass as predicted by the ODIM hypothesis. Our data suggest no direct explanations for individual-level variation. Variation in digestive status could translate into significant variation in respiration rate (see Fig. 1). However, this seems an unlikely explanation because larvae had continuous access to food and only growth-period observations were included in the individual-level analyses, which probably means that no larva was even close to attaining the post-absorptive state (i.e. ca. 3 h of starvation; Fig. 1).

Furthermore, for variation in digestive status to translate into divergent trends among individuals, each individual should consistently be in its characteristic digestive state at several successive measurements, which seems very unlikely, especially as the measurement times were not fixed.

To conclude, we found support for the ODIM hypothesis in the penultimate larval instar but not in the final instar in a non-model lepidopteran, *P. napi*. Data on the penultimate instar suggest that oxygen limitation may emerge gradually, as no abrupt change in the relationship between respiration (metabolic) rate and mass was observed. Gradually emerging oxygen limitation would suggest that there is no sharp point – critical mass (i.e. critical mass as defined by the ODIM hypothesis) – at which oxygen supply triggers moulting, but oxygen supply may, at a certain threshold, trigger other mechanisms that result in an exact critical mass. It also remains possible that the critical mass is rather 'a critical window of mass' during which moult induction gradually takes place. Although our data suggest gradual oxygen limitation at the population level, the pattern may be different at the individual level. This is because individual-level analysis in the final larval instar (Fig. 4) suggests different patterns at the individual and population levels. The benefits of our novel methodology are evident as we could reveal variation at different levels, and appropriately test the predictions of the ODIM hypothesis by only including periods when larvae are actually growing. Compared with the earlier population-level study with *M. sexta* in which no inter-instar differences were found in relation to the ODIM hypothesis (Callier and Nijhout, 2011), the lack of support in final-instar *P. napi* is contradictory. As stated above, we cannot currently completely refute the ODIM hypothesis for final-instar *P. napi* because of individual-level variation. More species and more instars must be studied, with a particular focus on individual-level variation, before we can make any generalisations concerning the ODIM hypothesis. Also, the possibility that moults between larval instars are triggered by a different mechanism compared with the final metamorphic (pupal) moult warrants further studies, even though data on *M. sexta* suggest a similar mechanistic basis in both cases (Callier and Nijhout, 2011).

Acknowledgements
We thank two anonymous reviewers for their constructive comments on an earlier version of the manuscript.

Competing interests
The authors declare no competing or financial interests.

Author contributions
S.M.K., P.L. and K.G. designed the study, S.M.K. and P.L. conducted the experiment, S.M.K. and P.L. analyzed the data, and S.M.K., P.L. and K.G. wrote the paper.

Funding
This study was financed by the international fellowship program at Stockholm University (to S.M.K.), the Finnish Cultural Foundation (Suomen Kulttuurirahasto; to S.M.K.), the strategic research programme EkoKlim at Stockholm University (to K.G.), the Knut and Alice Wallenberg Foundation [Knut och Alice Wallenbergs Stiftelse; grant no. 2012.00558 to K.G.] and the Swedish Research Council [Vetenskapsrådet; grant no. 2012-3715, K.G. co-applicant].

Data availability
Data are available from the Dryad Digital Repository http://dx.doi.org/10.5061/dryad.dr559

Supplementary information
Supplementary information available online at
http://jeb.biologists.org/lookup/doi/10.1242/jeb.140442.supplemental

References
Bennet-Clark, H. C. (1963). The relation between epicuticular folding and the subsequent size of an insect. *J. Insect. Physiol.* **9**, 43-46.
Callier, V. and Nijhout, H. F. (2011). Control of body size by oxygen supply reveals size-dependent and size-independent mechanisms of molting and metamorphosis. *Proc. Natl. Acad. Sci. USA* **108**, 14664-14669.
Callier, V. and Nijhout, H. F. (2012). Supply-side constraints are insufficient to explain the ontogenetic scaling of metabolic rate in the tobacco hornworm, *Manduca sexta*. *PLoS ONE* **7**, e45455.
Callier, V. and Nijhout, H. F. (2013). Body size determination in insects: a review and synthesis of size- and brain-dependent and independent mechanisms. *Biol. Rev.* **88**, 944-954.
Callier, V. and Nijhout, H. F. (2014). Plasticity of insect body size in response to oxygen: integrating molecular and physiological mechanisms. *Curr. Opin. Insect Sci.* **1**, 59-65.
Callier, V., Shingleton, A. W., Brent, C. S., Ghosh, S. M., Kim, J. and Harrison, J. F. (2013). The role of reduced oxygen in the developmental physiology of growth and metamorphosis initiation in *Drosophila melanogaster*. *J. Exp. Biol.* **216**, 4334-4340.
Camp, A. A., Funk, D. H. and Buchwalter, D. B. (2014). A stressful shortness of breath: molting disrupts breathing in the mayfly *Cloeon dipterum*. *Freshw. Sci.* **33**, 695-699.
Davison, A. C. and Hinkley, D. V. (1997). *Bootstrap Methods and their Application*. New York, NY: Cambridge University Press.
Downer, R. (1981). *Energy Metabolism in Insects*. New York: Plenum Press.
Esperk, T. and Tammaru, T. (2004). Does the 'investment principle' model explain moulting strategies in lepidopteran larvae? *Physiol. Entomol.* **29**, 56-66.
Folch, J., Lees, M. and Sloane Stanley, G. H. (1957). A simple method for the isolation and purification of total lipids from animal tissue. *J. Biol. Chem.* **226**, 497-509.
Greenberg, S. and Ar, A. (1996). Effects of chronic hypoxia, normoxia and hyperoxia on larval development in the beetle *Tenebrio molitor*. *J. Insect Physiol.* **42**, 991-996.
Greenlee, K. J. and Harrison, J. F. (2004). Development of respiratory function in the American locust *Schistocerca americana* II. Within-instar effects. *J. Exp. Biol.* **207**, 509-517.
Greenlee, K. J. and Harrison, J. F. (2005). Respiratory changes throughout ontogeny in the tobacco hornworm caterpillar, *Manduca sexta*. *J. Exp. Biol.* **208**, 1385-1392.
Grunert, L. W., Clarke, J. W., Ahuja, C., Eswaran, H. and Nijhout, H. F. (2015). A quantitative analysis of growth and size regulation in *Manduca sexta*: the physiological basis of variation in size and age at metamorphosis. *PLoS ONE* **10**, e0127988.
Hahn, D. A. and Denlinger, D. L. (2007). Meeting the energetic demands of insect diapause: nutrient storage and utilization. *J. Insect Physiol.* **53**, 760-773.
Helm, B. R. and Davidowitz, G. (2013). Mass and volume growth of an insect tracheal system within a single instar. *J. Exp. Biol.* **216**, 4703-4711.
Kivelä, S. M., Friberg, M., Wiklund, C., Leimar, O. and Gotthard, K. (2016). Towards a mechanistic understanding of insect life history evolution: oxygen-dependent induction of moulting explains moulting sizes. *Biol. J. Linn. Soc.* **117**, 586-600.
Lease, H. M., Wolf, B. O. and Harrison, J. F. (2006). Intraspecific variation in tracheal volume in the American locust, *Schistocerca americana*, measured by a new inert gas method. *J. Exp. Biol.* **209**, 3476-3483.
Lighton, J. R. B. (2008). *Measuring Metabolic Rates: A Manual for Scientists*. New York, NY: Oxford University Press.
Lighton, J. R. B., Bartholomew, G. A. and Feener, D. H. (1987). Energetics of locomotion and load carriage and a model of the energy cost of foraging in the leaf-cutting ant *Atta colombica* Guer. *Physiol. Zool.* **60**, 524-537.
Muggeo, V. M. R. (2008). segmented: an R Package to fit regression models with broken-line relationships. *R News* **8**, 20-25. http://cran.r-project.org/doc/Rnews/.
Newman, H. A. I., Gordon, E. A., Heggen, D. W. and Keller, M. D. (1972). Rapid extraction of triglycerides from human adipose tissue with petroleum ether. *Clin. Chem.* **18**, 290-292.
Nielsen, M. G. and Christian, K. A. (2007). The mangrove ant, *Camponotus anderseni*, switches to anaerobic respiration in response to elevated CO_2 levels. *J. Insect Physiol.* **53**, 505-508.
Nijhout, H. F. and Williams, C. M. (1974). Control of moulting and metamorphosis in the tobacco hornworm, *Manduca sexta* (L.): growth of the last-instar larva and the decision to pupate. *J. Exp. Biol.* **61**, 481-491.
Nijhout, H. F., Davidowitz, G. and Roff, D. A. (2006). A quantitative analysis of the mechanism that controls body size in *Manduca sexta*. *J. Biol.* **5**, 16.
Nijhout, H. F., Roff, D. A. and Davidowitz, G. (2010). Conflicting processes in the evolution of body size and development time. *Philos. Trans. R. Soc. B Biol. Sci.* **365**, 567-575.

Nijhout, H. F., Riddiford, L. M., Mirth, C., Shingleton, A. W., Suzuki, Y. and Callier, V. (2014). The developmental control of size in insects. *Wiley Interdiscip. Rev. Dev. Biol.* **3**, 113-134.

Ojeda-Avila, T., Woods, H. A. and Raguso, R. A. (2003). Effects of dietary variation on growth, composition, and maturation of *Manduca sexta* (Sphingidae: Lepidoptera). *J. Insect Physiol.* **49**, 293-306.

Schmidt-Nielsen, K. (1991). *Animal Physiology*. Cambridge: Cambridge University Press.

Sears, K. E., Kerkhoff, A. J., Messerman, A. and Itagaki, H. (2012). Ontogenetic scaling of metabolism, growth, and assimilation: testing metabolic scaling theory with *Manduca sexta* larvae. *Physiol. Biochem. Zool.* **85**, 159-173.

Shingleton, A. W. (2011). Evolution and the regulation of growth and body size. In *Mechanisms of Life History Evolution: The Genetics and Physiology of Life History Traits and Trade-Offs* (ed. T. Flatt and A. Heyland), pp. 43-55. UK: Oxford University Press.

Warton, D. I., Duursma, R. A., Falster, D. S. and Taskinen, S. (2012). smatr 3 – an R package for estimation and inference about allometric lines. *Methods Ecol. Evol.* **3**, 257-259.

Wigglesworth, W. B. (1972). *The Principles of Insect Physiology*. London: Chapman and Hall.

Williams, C. M., Thomas, R. H., MacMillan, H. A., Marshall, K. E. and Sinclair, B. J. (2011). Triacylglyceride measurement in small quantities of homogenised insect tissue: comparisons and caveats. *J. Insect Physiol.* **57**, 1602-1613.

Zebe, E. (1953). Über den Respiratorischen Quotienten der Lepidoptera. *Naturwissenschaften* **40**, 298.